

Dinuclear lanthanoid(III) dithiocarbamate complexes bridged by (*E*)-*N*-benzylidenepicolinohydrazonate: Syntheses, crystal structures and spectroscopic properties

Abdallah Yakubu^a, Takayoshi Suzuki^{a,b,*}, Masakazu Kita^c

^a Graduate School of Natural Science and Technology, Okayama University, 3-1-1 Tsushima-Naka, Kita-ku, Okayama 700-8530, Japan

^b Research Institute for Interdisciplinary Science, Okayama University, 3-1-1 Tsushima-Naka, Kita-ku, Okayama 700-8530, Japan

^c Faculty of Education, Okayama University, 3-1-1 Tsushima-Naka, Kita-ku, Okayama 700-8530, Japan

ARTICLE INFO

Keywords:

Hydrazone
Dithiocarbamate
Crystal structures
Lanthanoid
Magnetic circular dichroism

ABSTRACT

(*E*)-*N*-Benzylidenepicolinohydrazide (Hbphz) was used to synthesize a series of hydrazone-bridged homodinuclear Ln^{III} dithiocarbamate (RR'dtc[−]) complexes of the form [$\{Ln(RR'dtc)_2\}_2(\mu\text{-bphz})_2$] {Ln = La, Pr, Nd, Sm or Eu; RR' = dimethyl-(Me₂) or pyrrolidine-(pyr)}. X-ray crystallographic studies revealed that these complexes possessed a common head-to-tail type dinuclear structural motif in which two hydrazone ligands bridged two Ln^{III} centers in the $\mu - 1 \kappa^2 N(\text{py}), O:2 \kappa^2 O, N(\text{imine})$ mode and two RR'dtc ligands coordinated to each Ln^{III} center. Interestingly, while the Sm^{III} and Eu^{III} complexes crystallized as simple 8:8-coordinate dinuclear molecules, the lighter Ln^{III} (i.e. La^{III}, Pr^{III} and Nd^{III}) complexes afforded in some cases 9:9-coordinate molecules, where the ninth coordination site was occupied by a solvent ethanol or methanol molecule. Even for the lighter Ln^{III} complexes, the complexes were solved in dichloromethane or chloroform as the 8:8-coordinate dimer, as revealed by ¹H NMR spectroscopy. In the UV–visible absorption and magnetic circular dichroism (MCD) spectra of the complexes, similar spectral patterns for ligand-centered and Laporte forbidden f–f transitions were observed. The MCD spectral studies demonstrated the characteristic magneto-optical behavior of the complexes.

1. Introduction

The coordination chemistry of hydrazones is an active research area in view of their general interests and application of hydrazone complexes [1,2]. Hydrazones can coordinate to a metal center either as neutral molecules or deprotonated anionic forms; therefore, the hydrazone complexes often exhibit interesting reversible properties dependent on the solvent acidity [3,4]. In addition, the exploitation of possible ligating substitutional groups affords a variety of coordination modes of the hydrazones which would give the complexes with interesting structural diversity, magnetic and spectroscopic properties [5].

Lanthanoid complexes of hydrazones are being investigated for potential applications in various fields including supramolecular assemblies and magnetic materials. Chandrasekhar et al. have prepared a series of hydrazone-based homodinuclear lanthanoid complexes and revealed the presence of weak antiferromagnetic coupling between the Ln^{III} centers at low temperature [6]. Thompson and co-authors have investigated the coordination chemistry of tritopic pyridinebis(hydrazone) with some Ln^{III} ions [7]. Klouras, Perlepes and their

collaborators characterized dinuclear 2-acetylpyridine-substituted hydrazone complexes with four bridging acetate groups [8]. The structural characterizations and magnetic properties of other hydrazone-based dinuclear Dy₂^{III} [9] and tetranuclear Ln₄^{III} [10] complexes have also been reported. In addition, several mixed-ligand lanthanoid complexes bearing hydrazones (or the deprotonated hydrazoneates) and β -diketonates (or other oxygen-donor ligands) have been reported; however, those of the analogous mixed-ligand complexes with dithiocarbamates have not yet been investigated. Lanthanoid dithiocarbamate compounds have important practical applications in catalysis, nanotechnology and microelectronics, and, therefore, their structural, thermodynamical and spectroscopic properties have been studied in detail [11,12]. So far, most of the mixed-ligand dithiocarbamate lanthanoid complexes studied involve 1,10-phenanthroline or 2,2'-bipyridine as an ancillary ligand.

In this study, a hydrazone derived from picolinohydrazide and benzaldehyde, (*E*)-*N*-benzylidenepicolinohydrazide (Hbphz) was synthesized and used to prepare a series of lanthanoid dithiocarbamate complexes (Scheme 1). The structural features and spectroscopic

* Corresponding author.

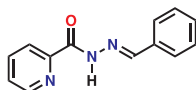
E-mail address: suzuki@okayama-u.ac.jp (T. Suzuki).

<https://doi.org/10.1016/j.ica.2019.119124>

Received 31 July 2019; Received in revised form 27 August 2019; Accepted 2 September 2019

Available online 04 September 2019

0020-1693/© 2019 Elsevier B.V. All rights reserved.



Scheme 1. (E)-N-benzylidenepicolinohydrazide (Hbphz).

properties of these hydrazone-bridged homodinuclear lanthanoid dithiocarbamate complexes were investigated.

2. Experimental section

2.1. Synthesis of (E)-N-benzylidenepicolinohydrazide (Hbphz)

2-Pyridinecarboxylic acid hydrazide (=picolinohydrazide) (343 mg, 2.5 mmol) was dissolved in ethanol (20 mL) and benzaldehyde (265 mg, 2.5 mmol) was added. The mixture was stirred for 3 h at room temperature and, then, allowed to stand overnight. A slight shaking of the mixture triggered precipitation of the product. Analytically pure white fluffy product was isolated in 73% yield. Slow evaporation of a methanolic solution of the product yielded colorless needle-shaped crystals suitable for X-ray diffraction analysis. Anal. Found: C, 69.23; H, 4.67; N, 18.55%. Calcd. for $C_{13}H_{11}N_3O$: C, 69.32; H, 4.92; N, 18.66%. IR (KBr disc)/ cm^{-1} : $\nu(N-H)$, 3212; $\nu(C=O)$, 1664; $\nu(C=N)$, 1522; $\nu(N-N)$, 1141. 1H NMR (300 MHz, Chloroform- d , 22 °C): δ 10.99 (s, 1H), 8.58 (ddd, J = 4.8, 1.8, 0.9 Hz, 1H), 8.42–8.16 (m, 2H), 8.02–7.64 (m, 3H), 7.60–7.31 (m, 4H).

2.2. Synthesis of complexes

All complexes reported in this article were similarly prepared by a method described below. To a mixture of Hbphz (1.00 mmol) and Et_3N (1.00 mmol) in MeOH (10 mL) was added a methanolic solution (10 mL) of $LnX_3 \cdot 6H_2O$ (Ln = La, Pr, Nd, Sm or Eu; X^- = Cl^- or NO_3^-) (1.00 mmol) with stirring. $Na(Me_2dtc)$ or $NH_4(pyrdtc)$ (2.00 mmol) in MeOH (10 mL) was added. The mixture was stirred for 5 h at room temperature and the resulting precipitate was collected by filtration, washed with MeOH and dried in air. The crude product was purified by recrystallization from a dichloromethane or chloroform solution by layering of ethanol, methanol or diethyl ether. The analytical and FT-IR spectral data are given below.

2.2.1. $[La(Me_2dtc)_2]_2(\mu-bphz)_2$ (1a)

Pale green crystals were obtained from a mixture of CH_2Cl_2 and EtOH in 18% yield. Anal. Found: C, 36.29; H, 3.77; N, 11.21; S, 19.30%. Calcd. for $C_{38}H_{44}N_{10}O_2La_2S_8 \cdot 2CH_3OH \cdot 2H_2O$: C, 36.75; H, 4.32; N, 10.71; S, 19.62%. IR (KBr disc)/ cm^{-1} : $\nu(C=N)$, 1540; $\nu(N-N)$, 1161; $\nu(C-N)$, 1349; $\nu(C-S)$ 982.

2.2.2. $[La(pyrdtc)_2]_2(\mu-bphz)_2$ (1b)

Pale green crystals were obtained from a mixture of $CHCl_3$ and EtOH in 21% yield. Anal. Found: C, 40.55; H, 3.99; N, 10.37; S, 18.65%. Calcd. for $C_{46}H_{52}N_{10}O_2La_2S_8 \cdot CH_3OH \cdot 2H_2O$: C, 40.92; H, 4.38; N, 10.15; S, 18.60%. IR (KBr disc)/ cm^{-1} : $\nu(C=N)$, 1539; $\nu(N-N)$, 1163; $\nu(C-N)$, 1430; $\nu(C-S)$ 1005.

2.2.3. $[Pr(Me_2dtc)_2]_2(\mu-bphz)_2$ (2a)

Green crystals were obtained from a mixture of CH_2Cl_2 and EtOH in 19% yield. Anal. Found: C, 37.23; H, 3.50; N, 11.41; S, 19.85%. Calcd. for $C_{38}H_{44}N_{10}O_2Pr_2S_8 \cdot 0.5CH_2Cl_2$: C, 36.89; H, 3.62; N, 11.17; S, 20.46%. IR (KBr disc)/ cm^{-1} : $\nu(C=N)$, 1540; $\nu(N-N)$, 1158; $\nu(C-N)$, 1347; $\nu(C-S)$ 979.

2.2.4. $[Pr(pyrdtc)_2]_2(\mu-bphz)_2$ (2b)

Green crystals were obtained from CH_2Cl_2 and EtOH in 21% yield. Anal. Found: C, 41.49; H, 4.25; N, 9.86; S, 18.90%. Calcd. for $C_{46}H_{52}N_{10}O_2Pr_2S_8 \cdot 2H_2O$: C, 40.88; H, 4.18; N, 10.37; S, 18.98%. IR

(KBr disc)/ cm^{-1} : $\nu(C=N)$, 1540; $\nu(N-N)$, 1163; $\nu(C-N)$, 1430; $\nu(C-S)$ 1006.

2.2.5. $[Nd(Me_2dtc)_2]_2(\mu-bphz)_2$ (3a)

Pale green crystals were obtained from $CHCl_3$ and MeOH mixture in 42% yield. Anal. Found: C, 36.82; H, 3.70; N, 11.16; S, 18.87%. Calcd. for $C_{38}H_{44}N_{10}O_2Nd_2S_8 \cdot 2CH_3OH \cdot 0.5CHCl_3$: C, 36.26; H, 3.95; N, 10.44; S, 19.12%. IR (KBr disc)/ cm^{-1} : $\nu(C=N)$, 1543; $\nu(N-N)$, 1159; $\nu(C-N)$, 1349; $\nu(C-S)$ 980.

2.2.6. $[Nd(pyrdtc)_2]_2(\mu-bphz)_2$ (3b)

Pale green crystals were obtained from CH_2Cl_2 and EtOH mixture in 43% yield. Anal. Found: C, 41.56; H, 4.56; N, 9.78; S, 17.57%. Calcd. for $C_{46}H_{52}N_{10}O_2Nd_2S_8 \cdot 2CH_3CH_2OH \cdot CH_2Cl_2 \cdot H_2O$: C, 41.25; H, 4.62; N, 9.43; S, 17.27%. IR (KBr disc)/ cm^{-1} : $\nu(C=N)$, 1541; $\nu(N-N)$, 1163; $\nu(C-N)$, 1431; $\nu(C-S)$ 1007. 1H NMR (300 MHz, Chloroform- d , 22 °C) δ 9.56 (dd, J = 14.6, 7.2 Hz, 1H), 8.94–8.23 (m, 2H), 7.99–7.70 (m, 1H), 7.69–7.37 (m, 1H), 7.26 (s, 1H), 4.39–3.40 (m, 8H), 1.67–1.04 (m, 8H).

2.2.7. $[Nd(pyrdtc)_2]_2(\mu-bphz)_2$ (3b')

Pale green crystals were obtained from CH_2Cl_2 and Et_2O . Anal. Found: C, 41.58; H, 4.00; N, 10.56; S, 19.20%. Calcd. for $C_{46}H_{52}N_{10}O_2Nd_2S_8$: C, 41.79; H, 3.96; N, 10.60; S, 19.40%. IR (KBr disc)/ cm^{-1} : $\nu(C=N)$, 1544; $\nu(N-N)$, 1163; $\nu(C-N)$, 1436; $\nu(C-S)$ 1004. 1H NMR (300 MHz, Chloroform- d , 22 °C) δ 9.56 (t, J = 10.2 Hz, 1H), 8.89–8.21 (m, 2H), 7.77 (t, J = 8.7 Hz, 1H), 7.69–7.37 (m, 1H), 7.26 (s, 2H), 4.27–3.47 (m, 6H), 1.61–1.03 (m, 6H).

2.2.8. $[Sm(Me_2dtc)_2]_2(\mu-bphz)_2$ (4a)

Pale yellow crystals were obtained from $CHCl_3$ and EtOH in 18% yield. Anal. Found: C, 35.97; H, 3.33; N, 10.93; S, 20.37%. Calcd. for $C_{38}H_{44}N_{10}O_2Sm_2S_8 \cdot 0.5CHCl_3$: C, 35.85; H, 3.48; N, 10.86; S 19.89%. IR (KBr disc)/ cm^{-1} : $\nu(C=N)$, 1545; $\nu(N-N)$, 1129; $\nu(C-N)$, 1351; $\nu(C-S)$ 982.

2.2.9. $[Sm(pyrdtc)_2]_2(\mu-bphz)_2$ (4b)

Pale yellow crystals were obtained from CH_2Cl_2 and EtOH in 22% yield. Anal. Found: C, 40.69; H, 3.71; N, 10.36; S, 19.06%. Calcd. for $C_{46}H_{52}N_{10}O_2Sm_2S_8 \cdot 0.5CH_2Cl_2$: C, 40.57; H, 3.88; N, 10.17; S, 18.63. IR (KBr disc)/ cm^{-1} : $\nu(C=N)$, 1545; $\nu(N-N)$, 1164; $\nu(C-N)$, 1437; $\nu(C-S)$ 1005.

2.2.10. $[Eu(Me_2dtc)_2]_2(\mu-bphz)_2$ (5a)

Orange crystals were obtained from $CHCl_3$ and MeOH in 37% yield. Anal. Found: C, 35.12; H, 3.41; N, 10.55; S, 19.20%. Calcd. for $C_{38}H_{44}N_{10}O_2Eu_2S_8 \cdot CHCl_3$: C, 35.04; H, 3.39; N, 10.48; S, 19.19%. IR (KBr disc)/ cm^{-1} : $\nu(C=N)$, 1545; $\nu(N-N)$, 1131; $\nu(C-N)$, 1351; $\nu(C-S)$ 982.

2.2.11. $[Eu(pyrdtc)_2]_2(\mu-bphz)_2$ (5b)

Orange crystals were obtained from $CHCl_3$ and EtOH in 40% yield. Anal. Found: C, 38.03; H, 3.70; N, 9.41; S, 17.23%. Calcd. for $C_{46}H_{52}N_{10}O_2Eu_2S_8 \cdot CHCl_3$: C, 38.76; H, 3.67; N, 9.62; S, 17.61%. IR (KBr disc)/ cm^{-1} : $\nu(C=N)$, 1545; $\nu(N-N)$, 1165; $\nu(C-N)$, 1436; $\nu(C-S)$ 1005.

2.3. Physical measurements

C, H, N and S analysis were carried out on a Perkin Elmer Series II CHNS/O Analyzer 2400 at Department of Instrumental Analyses, Advanced Science Research Center, Okayama University. The FT-IR spectra were recorded on a JASCO FT-001 FT-IR spectrophotometer by a KBr disc method in the 400–4000 cm^{-1} range. The UV–visible absorption spectra of the complexes in dichloromethane were obtained on a JASCO V-550 UV/VIS spectrophotometer at room temperature. Room temperature magnetic circular dichroism (MCD) spectra were measured

on a JASCO J-1500 CD spectropolarimeter equipped with a home-made neodymium magnet apparatus (ca. 0.5 T magnetic field) [13].

2.4. X-ray crystallographic study

X-ray diffraction intensity data were collected on a Rigaku R-Axis Rapid diffractometer, except for those of compound **5b** which were obtained on a Rigaku VariMax diffractometer with a Saturn-70 CCD detector, using graphite or multi-layered mirror monochromated Mo K α ($\lambda = 0.71075$ Å) radiation. The diffraction data were processed using the PROCESS-AUTO or CrystalClear software package [14] and the numerical absorption corrections were applied [15]. The structures were solved by the direct method employing the SIR2008 [16] or SHELXT [17] software package and expanded using Fourier techniques, and refined on F^2 (with all independent reflections) using SHELXL Version 2014/7 software package [18]. All non-hydrogen atoms were refined anisotropically. Hydrogen atoms were introduced at the theoretical positions and refined using riding models. All calculations were performed using the CrystalStructure software package [19].

3. Results and discussion

3.1. Synthesis and characterization of (*E*)-*N*-benzylidenepicolinohydrazide (Hbphz)

The hydrazone, Hbphz, was synthesized by a one-pot condensation reaction of equimolar amounts of 2-pyridinecarboxylic acid hydrazide and benzaldehyde in ethanol in 73% yield [20,21]. The product was characterized by elemental analysis, X-ray diffraction analysis, and IR and ^1H NMR spectroscopy. The ^1H NMR spectrum (Fig. 1a) suggested that the isolated hydrazone was a single product of possible *E* and *Z* isomers. The X-ray crystallographic analysis (Table S1) revealed the molecular structure of Hbphz as an *E*-isomer, which is depicted in Fig. 2a. The molecule has an almost planar structure; the planes of the pyridyl (N1, C1–C5) and phenyl (C8–C13) rings form a dihedral angle of $10.4(1)^\circ$. The plane defined by the central hydrazone linkage, $-\text{C}=\text{N}-\text{N}-\text{C}(=\text{O})-$, is tilted by $8.0(1)$ and $16.4(1)^\circ$, respectively, to the planes of the pyridyl and phenyl rings. The hydrazone $\text{C6}=\text{O1}$ bond

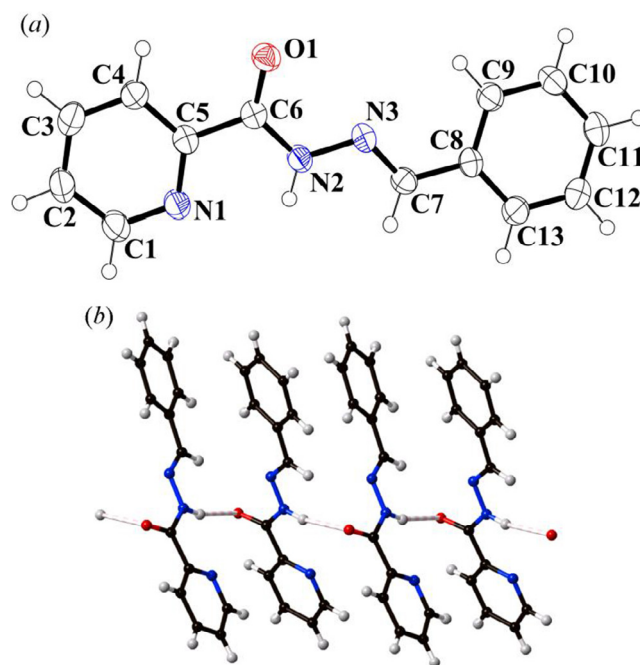


Fig. 2. (a) An ORTEP drawing of Hbphz (at 50% probability level), and (b) hydrogen-bonding interaction in the crystal of Hbphz.

length, $1.226(3)$ Å, indicates a ketonic character [7], and the imine $\text{N3}=\text{C7}$ bond length, $1.279(3)$ Å, shows its double bond character, while the $\text{N2}-\text{N3}$ and $\text{N2}-\text{C6}$ bond lengths are $1.381(2)$ and $1.356(3)$ Å, respectively. Therefore, the N2 atom should have an amide-H atom. Intermolecular $\text{N}-\text{H}\cdots\text{O}$ hydrogen bonds form a one-dimensional chain structure (Fig. 2b), running along the *b* axis. The UV-visible absorption spectra of Hbphz (Fig. S1) showed a characteristic intense band due to the $\pi \rightarrow \pi^*$ transition centered at 306 nm.

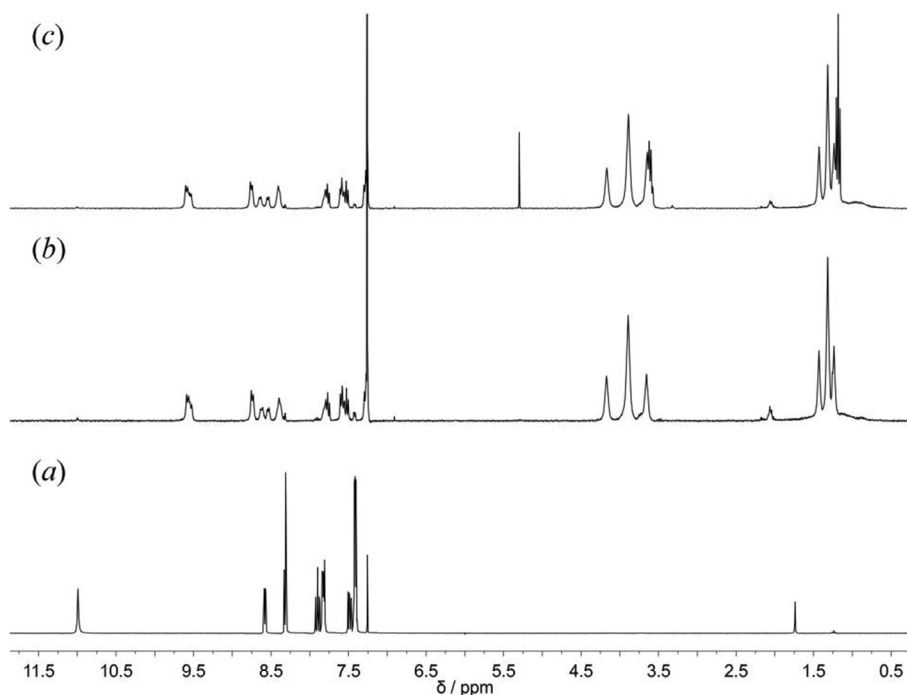
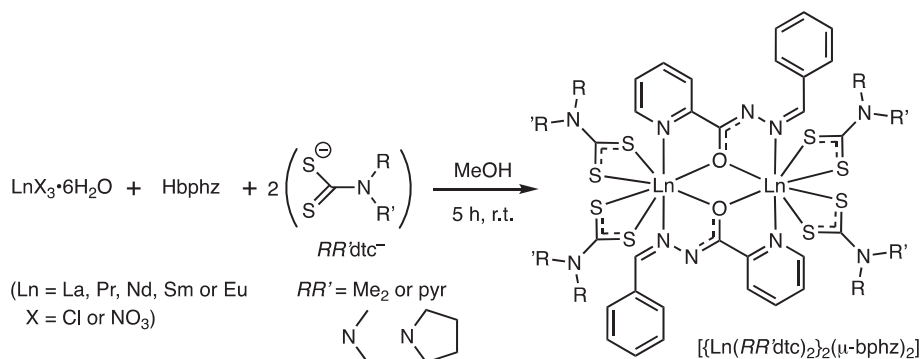


Fig. 1. ^1H NMR (300 MHz, Chloroform-*d*) spectra of (a) Hbphz, (b) $[\text{Nd}(\text{pyrdtc})_2]_2(\mu\text{-bphz})_2$ and (c) $[\text{Nd}(\text{pyrdtc})_2(\text{EtOH})]_2(\mu\text{-bphz})_2$.



Scheme 2. Synthetic route of the bphz-bridged complexes.

3.2. Synthesis and characterization of Ln^{III} complexes with the hydrazonate, bphz[−]

A reaction of Hbphz, LnX₃·6H₂O (Ln = La, Pr, Nd, Sm or Eu; X = Cl[−] or NO₃[−]), and sodium dimethyldithiocarbamate {Na(Me₂dtc)} or ammonium pyrrolidinedithiocarbamate {NH₄(pyrdtc)} in a 1:1:2 M ratio in the presence of Et₃N in methanol at room temperature gave a pale-yellow or green precipitate of the respective Ln^{III}(bphz)(RR'dtc)₂ complexes {Ln = La (**1x**), Pr (**2x**), Nd (**3x**), Sm (**4x**) or Eu (**5x**); RR' = Me₂ (**x = a**) or pyr (**x = b**)} (Scheme 2). Recrystallization of each product from dichloromethane (or chloroform) and ethanol (or methanol) afforded single-crystals suitable for the X-ray diffraction study. The elemental analysis of these products suggested the composition of Ln(bphz)(RR'dtc)₂·*n*(solvent).

Fig. S2 showed the FT-IR spectra of Hbphz and its complexes **3b** and **5b** as representative examples; other pyrdtc complexes of **1b**, **2b** and **4b** gave a similar spectral pattern. Also, the Me₂dtc complexes **1a–5a** showed similar IR spectra to one another. The ν(N–H) and ν(C=O) stretching bands appeared at 3212 cm^{−1} and 1664 cm^{−1}, respectively, in the spectrum of free Hbphz were disappeared in the spectra of the complexes, which indicated that the ligand has an anionic (i.e. bphz[−]) and enolate character [22]. The ν(C=N)_{imine} and ν(N–N) bands observed at 1522 and 1141 cm^{−1}, respectively, in the free Hbphz were shifted to higher wavenumber regions on complexation, suggesting the coordination of the imine-N donor to a Ln^{III} ion [1]. The ν(C–S) and ν(C–N) bands associated with the pyrdtc[−] ligand in the complexes appeared at 1007 and 1430 cm^{−1} in **3b** and 1005 and 1436 cm^{−1} in **5b**, respectively.

3.3. Crystal structure of the complexes

Further characterization of the bphz complexes, **1a–5b**, were performed by the single-crystal X-ray analysis. The crystallographic data are summarized in Table S1 in the Supporting Information. The selected structural parameters are listed in Table 1.

The Eu^{III}–pyrdtc complex, **5b**, was crystallized in a monoclinic space group Cc (with Z = 4), and the asymmetric unit contains two Eu^{III} ions, each of which attaches two bidentate S,S'-donating pyrdtc[−] ligands, two bridging bphz[−] (deprotonated hydrazonate) anions and three chloroform molecules of crystallization: [{Eu(pyrdtc)₂}]₂(μ-bphz)₂·3CHCl₃ (Fig. 3). The bphz[−] anions are bridged two Eu^{III} ions in a μ-1 κ²N(py), O:2 κ²O,N(imine) mode and form a head-to-tail type Eu₂(μ-bphz)₂ core. Each Eu^{III} center accomplishes a distorted dodecahedral 8-coordination geometry with N₂O₂S₄ donor atoms, and two pyrdtc ligands in the mutually pseudo-*trans* positions are almost coplanar and perpendicular to the Eu₂(bphz)₂ plane (Fig. 3b). Analogous Eu^{III}–Me₂dtc complex, **5a**, was crystallized in a triclinic space group P-1 with Z = 1 (based on the dinuclear unit). The asymmetric unit consists of an Eu^{III} ion, two bidentate S,S'-donating Me₂dtc[−] anions, and a bidentate N(py), O-bonding bphz[−] anion, but the symmetry expansion by

the crystallographic inversion center forms further coordination of the neighboring bphz[−] anion via a bidentate O,N(imine) mode. Thus, the molecule has a C_i symmetric (head-to-tail type) bphz-bridged dinuclear structure, as similar to the above pyrdtc complex: [{Eu(Me₂dtc)₂}]₂(μ-bphz)₂ (Fig. S3).

The Sm^{III}–Me₂dtc complex, **4a**, is isomorphous to that of **5a**, and a similar molecular structure is resulted: [{Sm(Me₂dtc)₂}]₂(μ-bphz)₂ (Fig. S4). In the case of Sm^{III}–pyrdtc complex of **4b**, a similar dinuclear molecular structure with two solvent CH₂Cl₂ molecules of crystallization, [{Sm(pyrdtc)₂}]₂(μ-bphz)₂·2CH₂Cl₂ (Fig. S5) was obtained in a triclinic space group P-1 with Z = 1 (based on the dinuclear unit).

All four complexes of Eu^{III} and Sm^{III}, **4a**, **4b**, **5a** and **5b**, have similar structural features with two Ln^{III} ions having a N₂O₂S₄ dodecahedral 8-coordination and two bridging monodeprotonated hydrazonate anions (bphz[−]). Compared to the metric parameters of the complexes with those of free Hbphz, the C=O and C–N bonds become longer (by ca. 0.07 Å) and shorter (by ca. 0.05 Å), respectively, while the N–N and N=C(imine) bond lengths are not different so much. This fact indicates that delocalization of the anionic character of the hydrazonate is limited in the [O=C–N] moiety, although the whole hydrazonate moiety [–C(=O)–N–N=C–] has a planar structure. Two Ln^{III} ions are placed on the hydrazonate planes, and the pyridine ring is also coplanar, while the phenyl ring of bphz[−] is slightly tilted from the planes (Table S2). Two RR'dtc ligands at each Ln^{III} ion are located above and below the Ln₂(μ-bphz)₂ plane, i.e., at mutually pseudo-*trans*-positions, and their coordination planes are almost parallel to each other but perpendicular to the Ln₂(μ-bphz)₂ plane. The coordination bond lengths around Eu^{III} or Sm^{III} centers are: Ln–S, 2.85–2.93 Å; Ln–N, 2.50–2.62 Å; Ln–O, 2.75–2.41 Å, the bite angles of RR'dtc are 61.8–62.5°, and the bridging angles of Ln–O–Ln are 112.2–113.6°.

In contrast to the above complexes, the La^{III} complexes of **1a** and **1b** were found to have a different molecular structure (Figs. 4 and S6, respectively) in the crystals. The Me₂dtc complex of **1a** was crystallized in a monoclinic space group P2₁/n with Z = 2 (based on the dinuclear unit), and the pyrdtc complex of **1b** was crystallized in a triclinic space group P-1 with Z = 1 (based on the dinuclear unit). Both complexes showed a dinuclear bphz-bridged La^{III}(μ-bphz)₂ structure having a crystallographic inversion center in the molecule. The bridging mode of the hydrazonate is the same as those in the Eu^{III} and Sm^{III} complexes, but the coordination bond lengths around the La^{III} are longer by 0.15–0.20 Å, which is consistent with the longer ionic radius of La^{III} than Eu^{III} and Sm^{III}. Because of the larger ionic size, the La^{III} center is deviated from the plane defined by two bridging ligands (Fig. 4b). In addition, the La^{III} center is coordinated by an ethanol molecule as well as two dithiocarbamate (RR'dtc[−]) ligands. The coordinated ethanol molecule is hydrogen-bonded to one of the S atoms of RR'dtc[−] ligand coordinated to the other La^{III} center (O2–H...S4: Fig. 4a). Two dithiocarbamate ligand planes are almost perpendicular to each other and to the bridging bphz ligand plane, and, therefore, the coordination geometry around each La^{III} center is characterized as a 9-coordinate

Table 1
Selected parameters of Ln^{III} complexes.^a

Parameters	1a	1b	2a	2b	3a(mol1) ^b	3a(mol2) ^{b,c}	3b	3b'	4a	4b	5a	5b
Bond Lengths (Å)												
Ln1–S1	3.002(3)	3.015(3)	2.906(4)	2.968(2)	2.920(3)	2.973(2)	2.990(2)	2.899(2)	2.856(5)	2.876(1)	2.853(3)	2.867(3)
Ln1–S2	3.031(3)	3.000(3)	2.921(3)	2.982(2)	2.895(3)	2.941(3)	2.992(2)	2.940(1)	2.863(6)	2.884(1)	2.844(3)	2.877(5)
Ln1–S3	3.032(3)	3.029(3)	2.919(3)	3.006(2)	2.898(3)	2.970(2)	2.963(2)	2.903(2)	2.893(6)	2.932(1)	2.857(3)	2.921(5)
Ln1–S4	3.052(3)	3.032(3)	2.889(4)	2.999(3)	2.889(2)	2.986(3)	2.952(2)	2.890(2)	2.870(5)	2.865(1)	2.870(3)	2.854(4)
Ln1–N1	2.695(8)	2.688(10)	2.658(9)	2.627(8)	2.629(7)	2.637(7)	2.620(7)	2.627(5)	2.620(13)	2.586(4)	2.589(7)	2.577(11)
Ln1–N3*	2.692(7)	2.702(10)	2.585(9)	2.639(7)	2.573(6)	2.624(7)	2.632(6)	2.589(6)	2.530(12)	2.560(4)	2.510(7)	2.498(10)
Ln1–O1	2.506(5)	2.520(6)	2.451(8)	2.480(4)	2.430(5)	2.456(5)	2.464(4)	2.409(5)	2.405(10)	2.375(3)	2.380(5)	2.390(7)
Ln1–O1*	2.518(6)	2.543(8)	2.488(10)	2.499(6)	2.432(5)	2.484(5)	2.483(5)	2.444(4)	2.410(8)	2.412(3)	2.398(6)	2.392(9)
Ln1–O2 _{EtOH}	2.583(7)	2.586(7)	–	2.549(6)	–	2.525(9) ^d	2.533(5)	–	–	–	–	–
C6–O1	1.297(9)	1.310(14)	1.294(13)	1.311(10)	1.312(9)	1.307(9)	1.286(9)	1.309(7)	1.301(17)	1.303(5)	1.297(10)	1.332(15)
C6–N2	1.332(10)	1.355(13)	1.329(17)	1.332(9)	1.329(10)	1.281(10)	1.329(8)	1.295(9)	1.327(16)	1.298(6)	1.302(9)	1.300(14)
Bond angles (°)												
S1–Ln1–S2	58.43(9)	58.57(8)	61.32(12)	59.30(6)	61.30(7)	59.44(9)	59.27(7)	61.58(5)	62.04(15)	62.12(3)	62.48(9)	62.35(11)
S3–Ln1–S4	57.63(8)	58.30(9)	61.38(11)	58.94(7)	61.56(8)	59.69(6)	59.74(6)	62.11(5)	61.79(14)	61.90(4)	62.15(8)	62.02(10)
Ln1–O1–Ln1*	115.48(19)	114.7(3)	111.9(3)	115.7(2)	113.3(2)	116.11(19)	115.5(2)	113.1(2)	112.2(4)	113.6(1)	112.9(2)	113.5(3)
Average Bond length (Å)												
Ln–S	3.029(4)	3.019(4)	2.909(7)	2.989(5)	2.900(4)	2.967(4)	2.974(4)	2.908(3)	2.871(1)	2.889(3)	2.856(6)	2.8798(9)
Ln–N	2.694(11)	2.695(14)	2.622(13)	2.633(11)	2.601(10)	2.631(11)	2.626(9)	2.608(8)	2.575(18)	2.573(6)	2.510(10)	2.538(15)
Ln–O	2.512(8)	2.532(10)	2.470(13)	2.490(7)	2.431(7)	2.470(7)	2.474(6)	2.427(6)	2.408(13)	2.394(4)	2.389(8)	2.391(21)
Bond angles (°)												
S–Ln1–S	58.03(12)	58.44(12)	61.35(16)	59.12(9)	61.43(10)	59.57(11)	59.51(9)	61.85(7)	61.9(2)	62.01(5)	62.3(12)	62.17(15)

^a The asterisk (*) indicates the symmetry-related atom.

^b Mol1 and mol2 have 8:8- and 9:9-coordinate structures, respectively.

^c Atom-numberings of mol2 should be modified appropriately: see Fig. 5 and Supplementary Information for details.

^d Ln2–O3_{MeOH}.

tricapped trigonal prism.

Since the La^{III}(RR'dtc)₂ fragments form a 9-coordinate dinuclear bphz-bridged complex with a coordinated EtOH ligand, while the corresponding Sm^{III} and Eu^{III} ones gave an 8-coordinate dinuclear complexes where two dithiocarbamate ligand planes at each Ln^{III} center are co-planar, it is interesting to investigate the molecular structures of the Pr^{III} and Nd^{III} analogues. The Pr^{III}–pyrdtc complex of **2b** and the Nd^{III}–pyrdtc complex of **3b** were found to be isomorphous to the La^{III}–pyrdtc complex of **1b**, and a similar molecular structure with 9-coordinate Pr^{III} ions (Fig. S7) or Nd^{III} ions (Fig. S8) resulted in. The structural characteristics of **2b** and **3b** are also the same as those of **1b**. The coordination bond lengths around Pr^{III} center in **2b** are slightly shorter than the corresponding ones around La^{III} in **1b** by 0.02–0.06 Å and those around Nd^{III} in **3b** are further shorter by ca. 0.01 Å, although the Pr^{III} and Nd^{III} centers in **2b** and **3b** are still not on the plane of the

bridging bphz ligands (Figs. S7b and S8b).

The crystal structure of Pr^{III}–Me₂dtc complex, **2a**, was found to be rather different from the above examples. It was crystallized in a triclinic space group *P*–1 with *Z* = 4 (based on the dinuclear unit), and its asymmetric unit contains a whole molecule of bphz-bridged dinuclear Pr^{III} complex, two fragments of 'Pr^{III}(Me₂dtc)₂(bphz)' which gives a dinuclear bphz-bridged complex by symmetry operation, and four molecules of solvent CH₂Cl₂ molecules; thus, the crystals of **2a** can be assigned as [{Pr(Me₂dtc)₂}(μ-bphz)₂].2CH₂Cl₂. There are three kinds of crystallographically different dinuclear complexes, but all of them are found to be 8-coordinate around the Pr^{III} centers (Fig. S9). The characteristics of the molecular structures are also similar to those of the Sm^{III} and Eu^{III} complexes of **4a** and **5a**.

The Nd^{III}–Me₂dtc complex, **3a**, showed a further characteristic crystal structure (Fig. 5). It was crystallized in a triclinic space group *P*–1

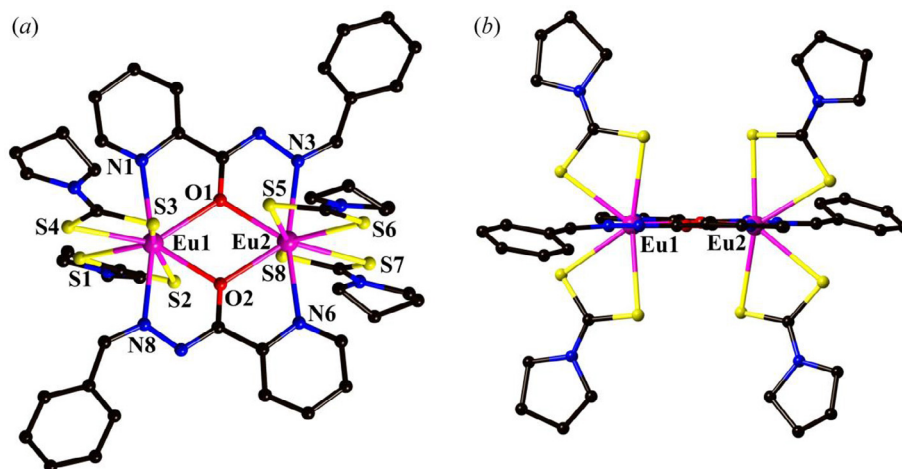


Fig. 3. (a) A perspective view of dinuclear complex of [Eu(pyrdtc)₂]₂(μ-bphz)₂ in **5b**·3CHCl₃ and (b) its side view from the Eu₂(bphz)₂ plane. Hydrogen atoms and lattice solvent molecules are omitted for clarity.

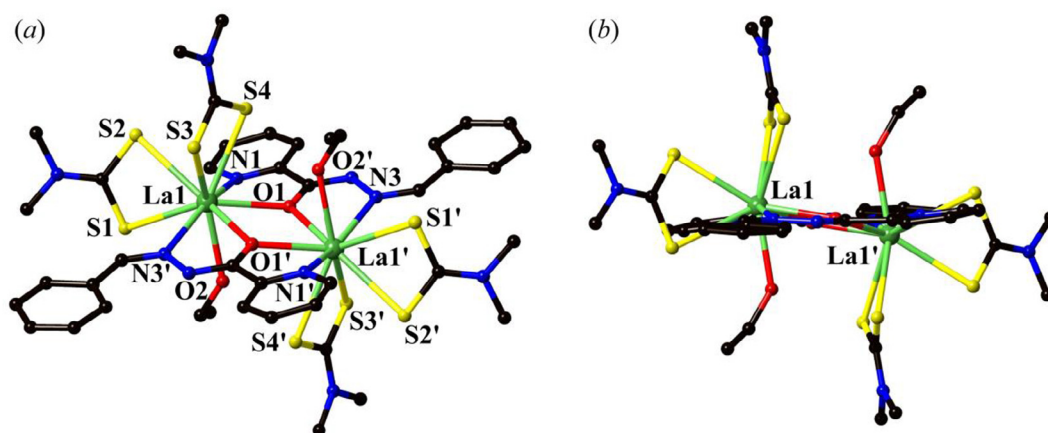


Fig. 4. (a) A perspective view of dinuclear complex of $[\{\text{La}(\text{Me}_2\text{dtc})_2(\text{EtOH})_2(\mu\text{-bphz})_2\}]$ in **1a** and (b) its side view from the $(\mu\text{-bphz})_2$ plane. Hydrogen atoms and lattice solvent molecules are omitted for clarity.

with $Z = 2$ (based on the dinuclear unit), and the asymmetric unit contains two halves of the dinuclear bphz-bridged Nd^{III} molecules and two solvent CHCl_3 molecules. Interestingly, these two fragments have different molecular structures; one of the molecules (with Nd1) has a similar 8-coordinate structure (Fig. 5a and b) to those of the Sm^{III} (**4a**) and Eu^{III} (**5a**) analogues (where two mutually *trans*-positioned Me_2dtc ligand planes are co-planar to each other), while the other molecule (with Nd2) is coordinated by an additional MeOH molecule to complete a 9-coordinate coordination geometry (Fig. 5c and d). Therefore, the crystals is assigned as $[\{\text{Nd}(\text{Me}_2\text{dtc})_2\}_2(\mu\text{-bphz})_2] \cdot [\{\text{Nd}(\text{Me}_2\text{dtc})_2(\text{MeOH})\}_2(\mu\text{-bphz})_2] \cdot 4\text{CHCl}_3$.

The above-mentioned crystallographic analyses suggested that the bphz-bridged dinuclear lanthanoid dithiocarbamate complexes tend to

form a 9-coordinate complex by a coordination of solvent EtOH (or MeOH) molecule used for recrystallization, when a larger Ln^{III} ion (e.g., La^{III} , Pr^{III} or Nd^{III}) was applied. Then, an interesting question arose; would an 8:8- or 9:9-coordinate molecule be obtained by recrystallizing these complexes from non-coordinating solvents? We have attempted several crystallization and finally isolated pale green and block single-crystals of the Nd^{III} -pyrdtc complex, **3b'**, from a mixture of dichloromethane and diethyl ether. Although the crystallinity was not good enough to obtain a satisfactory R value, we have confirmed the successful crystallization of the 8:8-coordinate $[\{\text{Nd}(\text{pyrdtc})_2\}_2(\mu\text{-bphz})_2]$ (**3b'**) complex (Table S1 and Fig. S10).

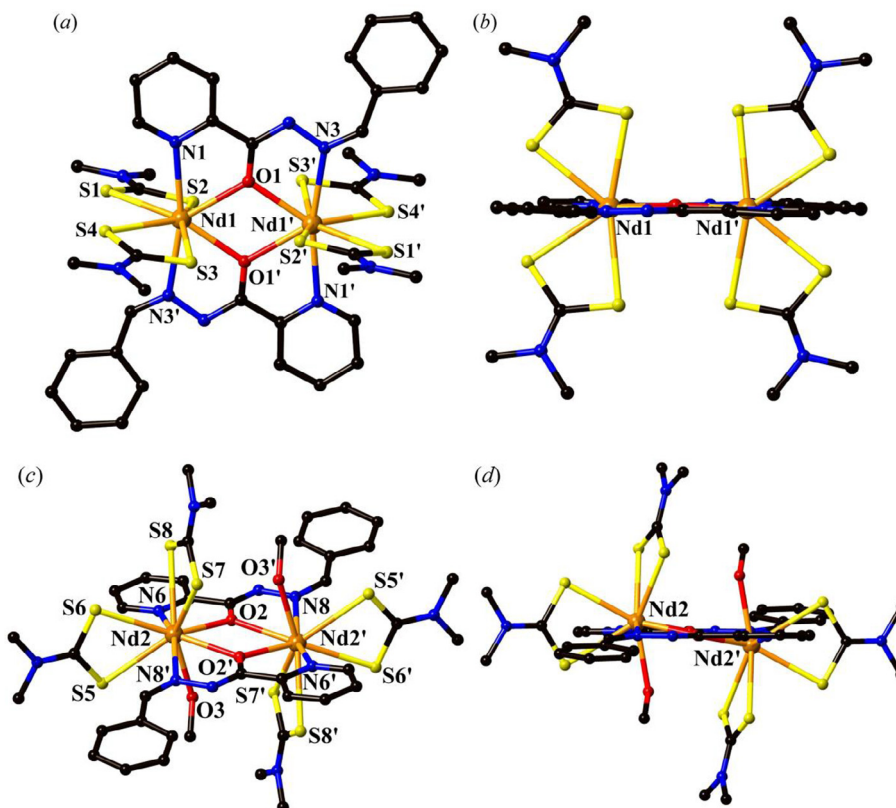


Fig. 5. Perspective views of (a and b) a 8:8-coordinate dinuclear complex of $[\{\text{Nd}(\text{Me}_2\text{dtc})_2\}_2(\mu\text{-bphz})_2]$ and (c and d) a 9:9-coordinate dinuclear complex of $[\{\text{Nd}(\text{Me}_2\text{dtc})_2(\text{MeOH})\}_2(\mu\text{-bphz})_2]$ in **3a** (b and d are their side views from the $(\mu\text{-bphz})_2$ plane). Hydrogen atoms and lattice solvent molecules are omitted for clarity.

3.4. Spectroscopic properties

3.4.1. ^1H NMR study

The ^1H NMR spectra of Hbphz and some Ln^{III} complexes in chloroform- d were measured. As representative examples, the spectra of free Hbphz and the Nd^{III} -pyrdtc complexes with 9:9- and 8:8-coordinate structures, $[\{\text{Nd}(\text{pyrdtc})_2(\text{EtOH})\}_2(\mu\text{-bphz})_2]$ (**3b**) and $[\{\text{Nd}(\text{pyrdtc})_2\}_2(\mu\text{-bphz})_2]$ (**3b'**), which were obtained by recrystallization from dichloromethane/ethanol and dichloromethane/diethyl ether, respectively, are shown in Fig. 1. In the spectrum of free Hbphz (bottom), the amide (NH) and imine ($\text{N}=\text{CH}$) proton resonances are observed at δ 10.99 and 8.58, respectively. In addition, multiplet resonances due to the aromatic (CH) protons are observed in the range of δ 7.31–8.42. The Nd^{III} complexes gave relatively sharp resonances in the typical range (δ 10–0) for diamagnetic compounds (middle and top), although they contain Nd^{III} ions. In these spectra, the disappearance of the amide NH resonance indicates the deprotonation from the hydrazone. The resonance for the imine ($\text{N}=\text{CH}$) proton is observed at δ 9.56, while those for the aromatic (CH) protons occurred in the range of δ 7.26–8.94. The methylene (CH_2) protons of pyrdtc $^-$ ligands gave two pseudo triplets around δ 3.8 and 1.3. In addition, in the spectrum of **3b** three sharp resonances due to free ethanol are observed [23]. These spectral features of **3b** and **3b'** suggest that the EtOH (or MeOH) molecule in the 9:9-coordinate complex dissociates in a chloroform solution to exist as an 8:8-coordinate dinuclear bphz-bridged complex.

3.4.2. UV-visible absorption and MCD spectra

UV-visible absorption and MCD spectra of the pyrdtc $^-$ complexes, **1b–5b**, were measured in CH_2Cl_2 solutions. The complexes exhibited similar absorption spectral pattern in the UV region as shown in Fig. S11. The band at 340 nm was assigned to the intra-ligand charge transfer transition [24,25]. In the visible region, sharp but weak absorption bands and MCD signals characteristic of f-f transitions were observed in the complexes. The spectra are presented in Figs. 6–9 and discussed below.

The absorption spectrum of **2b** (Fig. 6, top) shows four sharp but

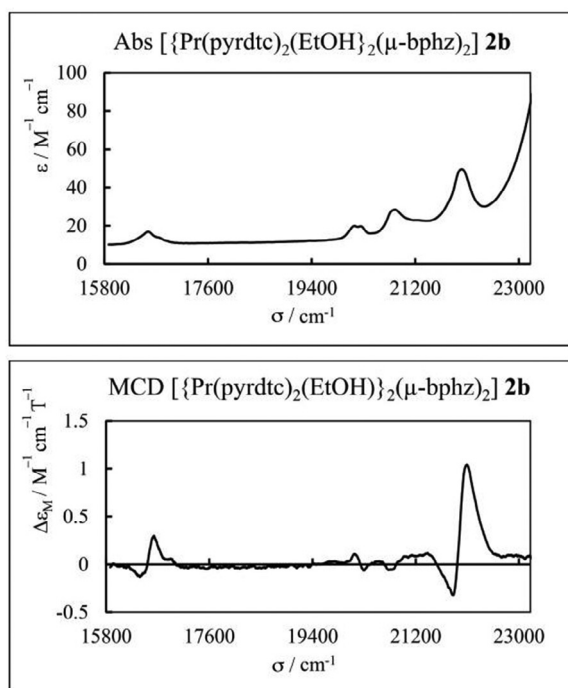


Fig. 6. Absorption (top) and MCD (bottom) spectra of $[\{\text{Pr}(\text{pyrdtc})_2(\text{EtOH})\}_2(\mu\text{-bphz})_2]$ **2b**.

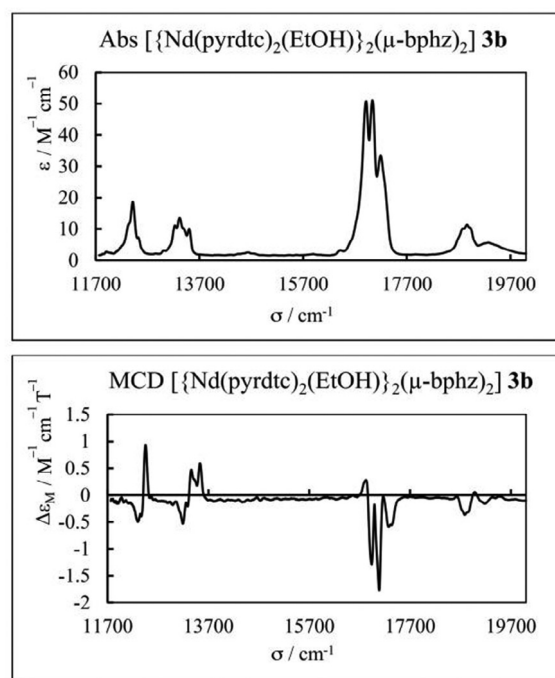


Fig. 7. Absorption (top) and MCD (bottom) spectra of $[\{\text{Nd}(\text{pyrdtc})_2(\text{EtOH})\}_2(\mu\text{-bphz})_2]$ **3b**.

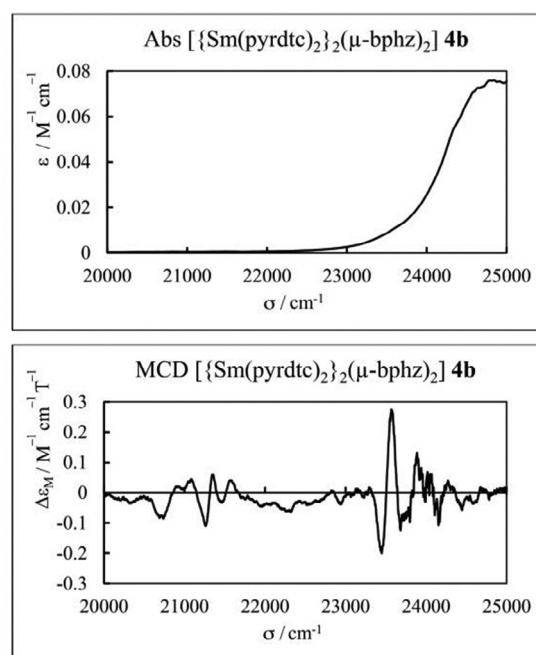


Fig. 8. Absorption (top) and MCD (bottom) spectra of $[\{\text{Sm}(\text{pyrdtc})_2\}_2(\mu\text{-bphz})_2]$ **4b**.

weak bands at 16,580, 20,200, 20,830 and 22,050 cm^{-1} . These bands are due to the f-f transition from the ground state $^3\text{H}_4$ to the $^1\text{D}_2$, $^3\text{P}_0$, ($^3\text{P}_1$, $^1\text{I}_6$) and $^3\text{P}_2$ excited states, respectively, which are based on the reported signal assignments for an aqueous $\text{Pr}(\text{NO}_3)_3$ and $\text{Pr}(\text{ClO}_4)_3$ solutions [26]. In the MCD spectrum (bottom), the f-f transition bands are observed as characteristic positive A-term MCD signals at 16,500 and 21,930 cm^{-1} , while negative A- and C-term MCD signals at 20,240 and 20,830 cm^{-1} , respectively.

The absorption spectrum (top) of complex **3b** (Fig. 7) shows four sharp but weak f-f bands with maximum peaks at 12,420, 13,320,

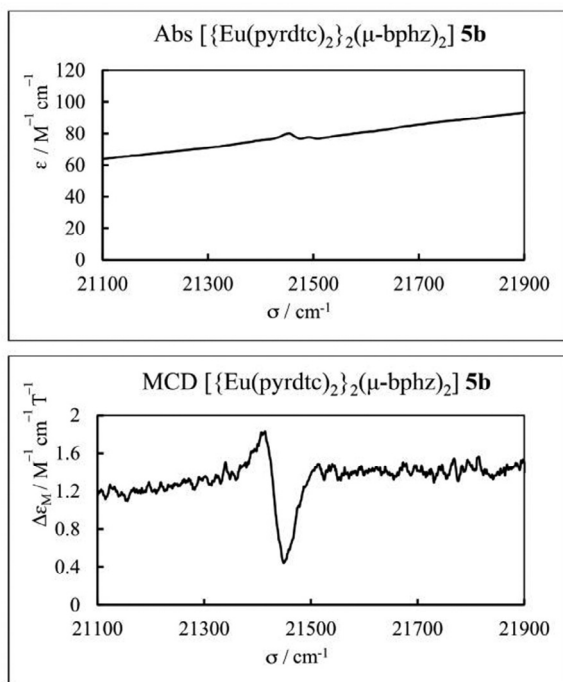


Fig. 9. Absorption (top) and MCD (bottom) spectra of $[\{\text{Eu}(\text{pyrdtc})_2\}_2(\mu\text{-bphz})_2]$ **5b**.

17,040 and 18,800 cm^{-1} , which are assigned to the $^4\text{I}_{9/2} \rightarrow (^4\text{F}_{5/2}, ^4\text{H}_{9/2})$, $(^4\text{S}_{3/2}, ^4\text{F}_{7/2})$, $(^2\text{G}_{7/2}, ^4\text{G}_{5/2})$ and $^4\text{G}_{7/2}$ transitions, respectively. The $^4\text{I}_{9/2} \rightarrow (^4\text{F}_{5/2}, ^4\text{H}_{9/2})$, $(^4\text{S}_{3/2}, ^4\text{F}_{7/2})$ and $(^2\text{G}_{7/2}, ^4\text{G}_{5/2})$ transitions occurred at slightly lower in energies than those of a similar hydrazone-based Nd^{III} complex reported by Singh et al. [27]. Compared to the related Nd^{III} complex with *N*-(furfuralidene)-*N*-isonicotinoylhydrazine [28], only the $^4\text{I}_{9/2} \rightarrow (^4\text{F}_{5/2}, ^4\text{H}_{9/2})$ band was consistent, and the other transitions occurred at lower energies. In the MCD spectrum (bottom), the MCD signals were observed at 12,380, 13,290, 13,500, 16,910 and 17,040 cm^{-1} . These signals are dominated by room temperature *C*-terms, except for the signal at 12,380 cm^{-1} which appeared as a positive pseudo *A*-term [29].

The characteristic $^4\text{I}_{9/2} \rightarrow (^4\text{G}_{5/2}, ^2\text{G}_{7/2})$ hypersensitive transition exhibits splitting at 16,910 and 17,040 cm^{-1} . These crystal-field splitting was also observed in the second derivative absorption spectra of $\text{Nd}(\text{C}_2\text{H}_3\text{O}_2)_3\cdot\text{H}_2\text{O}$ [30] and neodymium complex with feroxacin [31] at higher energies. The $^4\text{I}_{9/2} \rightarrow (^4\text{G}_{5/2}, ^2\text{G}_{7/2})$ hypersensitive transition *C*-term MCD signals are more clearly resolved in **3b** than those in previously reported mononuclear Nd^{III} analogues [29].

In Fig. 8 (top), no *f*-*f* bands were detected in the absorption spectrum for complex **4b** probably because they were overlapped or buried underneath the strong metal-ligand charge-transfer band around 24,000 cm^{-1} [28,32]. In the MCD spectrum (bottom), the structure of the MCD bands is very complicated due to the Zeeman splitting of the ground state and all the excited states [33]. Two characteristic MCD signals showing a positive *A*-term and a negative *C*-term occurred at 23,510 and 21,260 cm^{-1} , owing probably to the *f*-*f* transition from the $^6\text{H}_{6/2}$ ground state to the $^6\text{P}_{3/2}$ and $^4\text{I}_{13/2}$ excited states, respectively.

In Fig. 9 (top), complex **5b** exhibited two very weak bands at 21,450 and 21,460 cm^{-1} which would be assigned to the $^7\text{F}_0 \rightarrow ^5\text{D}_2$ transition. The positions of these bands are in good agreement, but the shapes are different from previously reported spectra of mononuclear $[\text{Eu}(\text{RR}'\text{dtc})_3(\text{NN})]$ ($\text{RR}' = \text{dimethyl-}, \text{pyrrolidine- and } S\text{-prolinol-}$; $\text{NN} = 1,10\text{-phenanthroline or } 2,2'\text{-bipyridine}$) complexes [29]. In the MCD spectrum (bottom), a negative pseudo *A*-term MCD signal is observed at 21,430 cm^{-1} and corresponds to the absorption bands. The shape of the negative pseudo *A*-term of **5b** is different from that of the

negative *B*-term observed in the previously reported mononuclear Eu^{III} dithiocarbamate complexes [29]. The MCD results show that the coordination environment of the lanthanoid with a mixed N,O,S donor set gives a significant difference in the electronic structure from that of an N,S donor set. This finding shows that the sensitivity of the MCD technique [34] can be used as an effective tool to probe the electronic structure(s) and physical properties of Ln^{III} complexes in solution.

4. Conclusion

A series of novel hydrazone-bridged homodinuclear Ln_2^{III} dithiocarbamate complexes were prepared and their crystal and molecular structures and spectroscopic properties were investigated. The crystal structures revealed that the early Ln^{III} ions tend to crystallize as a 9:9-coordinate complex with the ninth position occupied by a solvent alcohol molecule, while the middle Ln^{III} ions deposit the crystals of only 8:8-coordinate complex. The coordination of a deprotonated mono-anionic hydrazone ligand was confirmed by the IR and ^1H NMR spectroscopy. Similar spectral patterns of ligand-centered and Laporte forbidden *f*-*f* transitions were observed in the UV-visible spectral region. The MCD parameters exhibited by the complexes demonstrate their potential in magneto-optical applications. In addition, these hydrazone-bridged dinuclear lanthanoid(III) complexes with some suitable modification would be used as an effective building block for supramolecular chemistry. In particular, the late (heavier) Ln^{III} ions would be interesting in their magnetic and catalytic properties. Such an investigation of a series of complexes are now in progress in our laboratory.

Declaration of Competing Interest

The authors declare that they have no known competing financial interests or personal relationships that could have appeared to influence the work reported in this paper.

Acknowledgements

The authors wish to thank Dr. Yukinari Sunatsuki of his assistance in the crystallographic analysis. This work was supported by a Grant-in-Aid for Scientific Research No. 18K05146 from the Ministry of Education, Culture, Sports, Science, and Technology, Japan.

Appendix A. Supplementary data

Details of the crystal structures and the infrared and UV-visible absorption spectra of the complexes in PDF format. Crystallographic data for compounds **Hbphz** and complexes **1a–5b** have been deposited with the Cambridge Crystallographic Data Centre, CCDC 1944410–1944421. These data can be obtained free of charge from The Cambridge Crystallographic Data Centre via www.ccdc.cam.ac.uk/data_request/cif.

Supplementary data to this article can be found online at <https://doi.org/10.1016/j.ica.2019.119124>.

References

- [1] R.S. Baligar, V.K. Revankar, J. Serb. Chem. Soc. 71 (2006) 1301.
- [2] B. Moksharagni, K.H. Reddy, Eur. J. Biom. Pharm. Sci. 5 (2018) 810.
- [3] B. Parmar, K.K. Bisht, P. Maiti, P. Paul, E. Suresh, J. Chem. Sci. 126 (2014) 1373.
- [4] M. Chang, H. Horiki, K. Nakajima, A. Kobayashi, H.-C. Chang, M. Kato, Bull. Chem. Soc. Jpn. 83 (2010) 905.
- [5] A. Mori, T. Suzuki, Y. Sunatsuki, M. Kojima, Bull. Chem. Soc. Jpn. 88 (2015) 480.
- [6] S. Biswas, S. Das, G. Rogez, V. Chandrasekhar, Eur. J. Inorg. Chem. (2016) 3322.
- [7] M.U. Anwar, S.S. Tandon, L.N. Dawe, F. Habib, M. Murugesu, L.K. Thompson, Inorg. Chem. 51 (2012) 1028.
- [8] N.C. Anastasiadis, I. Mylonas-Margaritis, V. Psycharis, C.P. Raptopoulou, D.A. Kalofolias, C.J. Milios, N. Klouras, S.P. Perlepes, Inorg. Chem. Comm. 51 (2015) 99.

- [9] L. Zhang, Q.-Y. Zhang, P. Zhang, L. Zhao, M. Guo, J. Tang, *Inorg. Chem.* 56 (2017) 7882.
- [10] A. Gusev, R. Herchel, I. Nemec, V. Shul'gin, I.L. Eremenko, K. Lyssenko, W. Linert, Z. Trávníček, *Inorg. Chem.* 55 (2016) 12470.
- [11] W.M. Faustino, O.L. Malta, E.E.S. Teotonio, H.F. Brito, A.M. Simas, G.F. de Sá, *J. Phys. Chem. A* 110 (2006) 2510.
- [12] P. Pitchaimani, K.M. Lo, K.P. Elango, *Polyhedron* 93 (2015) 8.
- [13] A. Yakubu, T. Suzuki, M. Kita, *J. Chem. Educ.* 94 (2017) 1357.
- [14] (a) Rigaku Co. Ltd., *Process—Auto*, Akishima, Tokyo, 1998. (b) Rigaku Co., Ltd., *CrystalClear*, Akishima, Tokyo, 1998–2015.
- [15] Rigaku Co. Ltd., *NUMABS*, Akishima, Tokyo, 1999.
- [16] M.C. Burla, R. Caliandro, M. Camalli, B. Carrozzini, L.G. Cascarano, L. De Caro, C. Giacovazzo, G. Polidori, D. Siliqi, R. Spagna, *SIR2008*, *J. Appl. Cryst.* 40 (2007) 609.
- [17] M.G. Sheldrick, *SHELXT* Version 2014/5, *Acta Cryst. A* 70 (2014) C1437.
- [18] M.G. Sheldrick, *SHELXL* Version 2014/7, *Acta Cryst. A* 64 (2008) 112.
- [19] Rigaku Co. Ltd., *CrystalStructure* 4.3, Akishima, Tokyo, 2000–2018.
- [20] A. Mori, T. Suzuki, Y. Sunatsuki, A. Kobayashi, M. Kato, M. Kojima, K. Nakajima, *Eur. J. Inorg. Chem.* (2014) 186.
- [21] J. Qin, Q. Yin, S.-S. Zhao, J.-Z. Wang, S.-S. Qian, *Acta Chim. Slov.* 63 (2016) 55.
- [22] V.C. Havanur, D.S. Badiger, S.G. Ligade, K.B. Gudasi, *Der Pharm. Chem.* 3 (2011) 292.
- [23] P. Pitchaimani, M.L. Lo, K.P. Elango, *J. Coord. Chem.* 68 (2015) 2167.
- [24] M. Mahato, P.P. Jana, K. Harms, H.P. Nayek, *RSC Adv.* 5 (2015) 62167.
- [25] V. Vrdoljak, G. Pavlovic, T. Hrenar, M. Rubci, P. Siega, R. Dreos, M. Cindri, *RSC Adv.* 5 (2015) 104870.
- [26] C. Görller-Walrand, L. Fluyt, *Magnetic circular dichroism of lanthanides*, *Handb. Phys. Chem. Rare Earths* 40 (2010) 1–107.
- [27] B. Singh, T.B. Singh, *Indian J. Chem.* 38A (1999) 1286.
- [28] S.S. Devi, A.M. Singh, *J. Chem. Pharm. Res.* 3 (2011) 399.
- [29] A. Yakubu, T. Suzuki, M. Kita, *Inorg. Chim. Acta* 484 (2019) 394.
- [30] S.V.J. Lakshman, S. Buddhu, *Proc. Indian natn. Sci. Acad.* 47 A (6) (1981) 721.
- [31] N. Wang, W. Jiang, X. Xu, Z. Si, H. Bai, C. Tian, *Anal. Sci.* 18 (2002) 591.
- [32] C. Su, M. Tan, N. Tang, X. Gan, W. Liu, X. Wang, *J. Coord. Chem.* 38 (1996) 207.
- [33] C.E. Secu, S. Polosan, M. Secu, *J. Lumin.* 131 (2011) 1747.
- [34] K. Binnemans, *Coord. Chem. Rev.* 295 (2015) 1.